

Electronic supplementary information (ESI)

Synthesis, structural and spectroscopic characterization of zinc(II) iodide complex with 2-[(4-iodophenyl)iminomethyl]pyridine in the solid state and solution

Krzysztof Łyczko,^{*a} Monika Łyczko,^a Elżbieta Bednarek,^b Mehdi Khalaj,^c Karolina Węgrzyńska,^b Anna Baraniak,^b and Ingmar Persson^d

^a*Institute of Nuclear Chemistry and Technology, Dorodna 16, 03-195 Warsaw, Poland*

^b*National Medicines Institute, Chelmska 30/34, 00-725 Warsaw, Poland*

^c*Department of Chemistry, Buinzahra Branch, Islamic Azad University, Buinzahra, Iran*

^d*Department of Molecular Sciences, Swedish University of Agricultural Sciences, P.O. Box 7015, SE-750 07 Uppsala, Sweden*

*e-mail: k.lyczko@ichtj.waw.pl

Legends

Details of antibacterial studies

Fig. S1. IR spectrum of free L^{4-1} ligand.

Fig. S2. Experimental (black line) and simulated (red lines) IR spectra of $[ZnI_2(L^{4-1})]$ complex.

Table S1. $\pi\cdots\pi$ interactions for the studied complex (symmetry codes: (i) $x, -y+0.5, z+0.5$).

Table S2. Calculated transitions for $[ZnI_2(L^{4-1})]$ complex.

Fig. S3. UV-Vis spectra of $[ZnI_2(L^{4-1})]$ complex, free L^{4-1} ligand, and ZnI_2 in various solvents.

Fig. S4. Experimental (black) and TD-DFT/def2-TZVP/ECP(I)/IEFPCM(acetonitrile) simulated (red vertical lines) UV-Vis spectra of the $[ZnI_2(L^{4-1})]$ complex (calculated data were scaled by a factor of 0.88).

Fig. S5. The 1H NMR spectrum of $[ZnI_2(L^{4-1})]$ complex in CD_3CN (temp. $25^\circ C$).

Fig. S6. The ^{13}C NMR spectrum of $[ZnI_2(L^{4-1})]$ complex in CD_3CN (temp. $25^\circ C$).

Fig. S7. The 1H - ^{13}C HMBC spectrum of $[ZnI_2(L^{4-1})]$ complex in CD_3CN (temp. $25^\circ C$). The 1H and ^{13}C NMR spectra of the $[ZnI_2(L^{4-1})]$ complex are presented as projection spectra. The positions of the quaternary carbon atoms' signals: C2 (147.92 ppm), C1' (144.89 ppm), and C4' (96.65 ppm), which were not detected in the 1D ^{13}C NMR spectrum, are marked by the arrows.

Table S3. The experimental 1H and ^{13}C NMR chemical shifts δ [ppm] for free L^{4-1} ligand and $[ZnI_2(L^{4-1})]$ complex in CD_3CN (temp. $25^\circ C$, ref. to TMS, solvent: δ (1H) 1.941 ppm, δ (^{13}C) 1.51 ppm, 118.48 ppm).

Fig. S8. XANES spectra of the $[ZnI_2(L^{4-1})]$ complex registered in solid state (black line, no offset) and in various solvents: DMPU (brown line, offset 0.2), CH_2Cl_2 (purple, offset 0.4), acetonitrile (blue line, offset 1.0), methanol (orange line, offset 1.3), water (green line, offset 1.6), and DMSO (red line offset 2.0).

Table S4. MICs/MBC values (mg/L) and zone diameters of bacterial growth inhibition (mm) obtained for test compounds and ciprofloxacin for reference strains.

Details of antibacterial studies

The microdilution in broth and disk-diffusion methods were used to test the potency of the compounds. The minimum inhibitory concentrations (MICs) and minimum bactericidal concentrations (MBCs) were determined in the microdilution, while the inhibition zones of microbial growth were measured in the disk-diffusion method. The first assay consisted of preparing 2-fold dilutions of the substance in broth (from 512 mg/L to 0.5 mg/L), and the lowest concentration of the compound inhibiting visible bacterial growth was referred to as MIC, while the concentration causing inoculum death was called MBC. On the other hand, the second approach assessed the susceptibility of microorganisms to the tested compounds with a concentration of 5 µg in a disk. The obtained values were compared with those for ciprofloxacin, an antibiotic used in infections caused by all tested microbial species. The data interpretation for ciprofloxacin was performed using the European Committee on Antimicrobial Susceptibility Testing (EUCAST) guidelines (breakpoint tables for interpreting minimum inhibitory concentrations and zone diameters) [a].

[a] European Committee on Antimicrobial Susceptibility Testing. 2019. Breakpoints tables for interpretation of MICs and zone diameters. v 9.0. Available at <https://www.eucast.org>

Fig. S1 IR spectrum of free L^{4-} ligand.

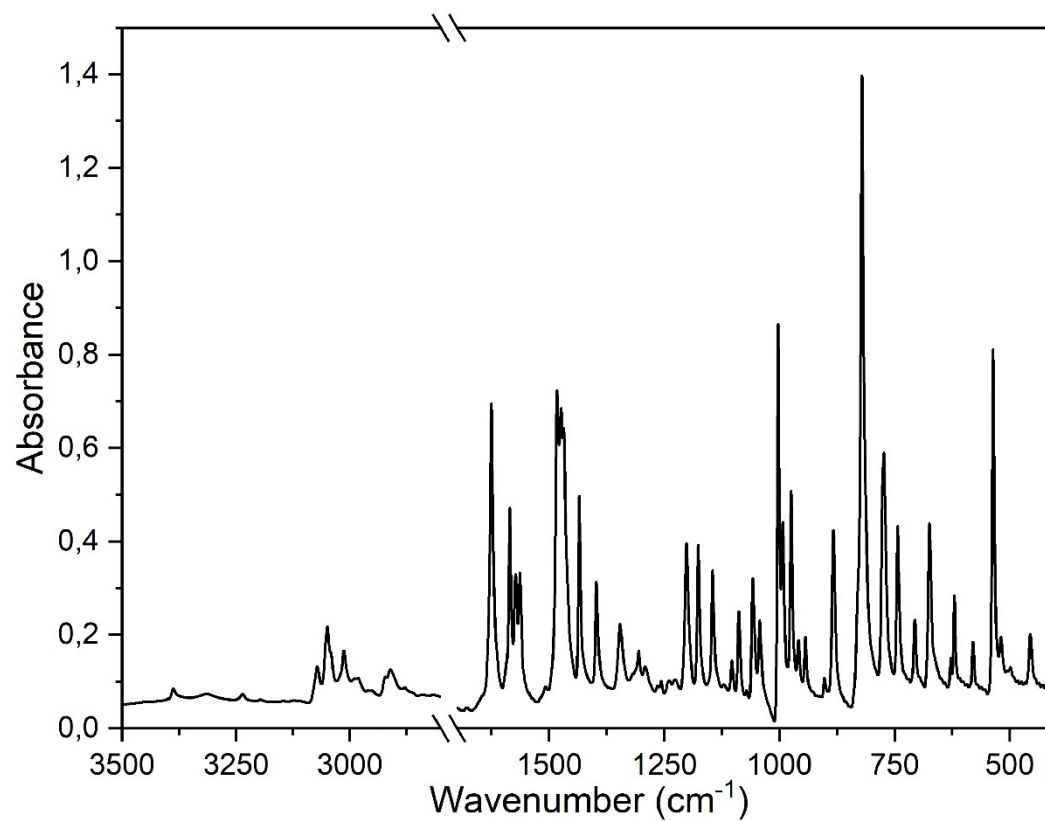


Fig. S2 Experimental (black line) and simulated (red lines) IR spectra of $[\text{ZnI}_2(L^{4-})]$ complex.

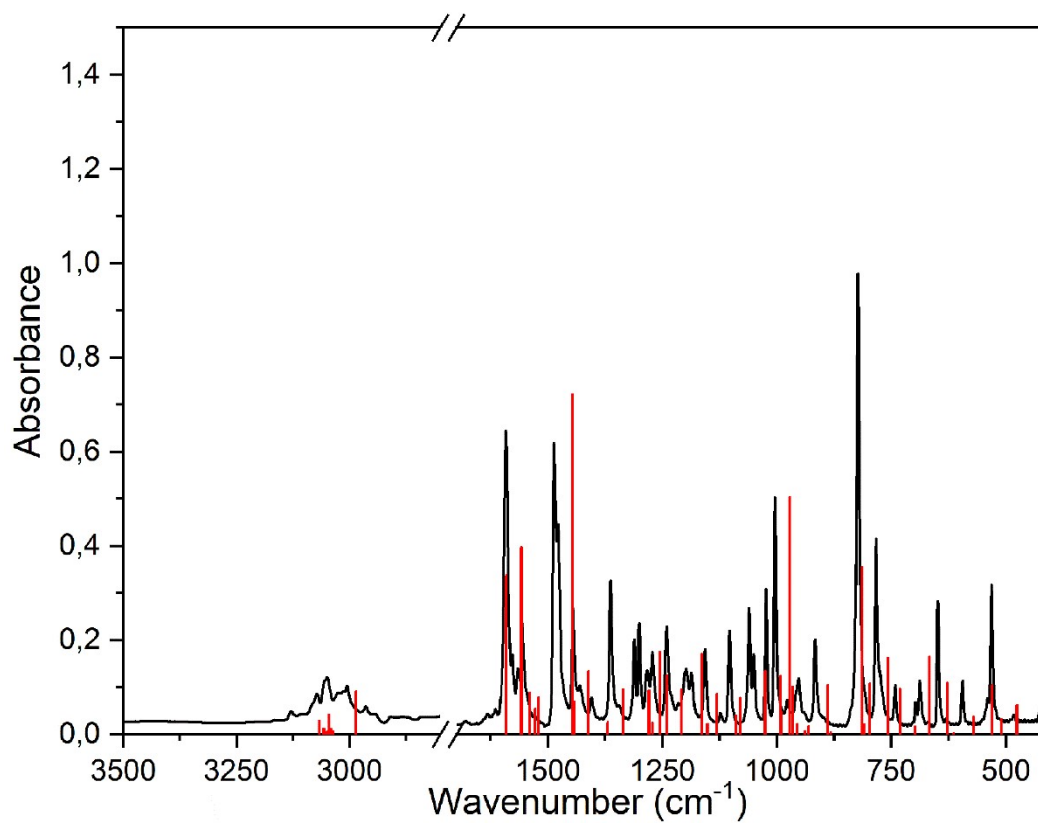


Table S1. $\pi\cdots\pi$ interactions for the studied complex (symmetry codes: (i) $x, -y+0.5, z+0.5$).

interaction	contact	distance (Å)
$\pi_{Ph}\cdots\pi_{py}$	C7 \cdots C3 ⁱ	3.372(5)
$\pi_{Ph}\cdots\pi_{py}$	C8 \cdots C2 ⁱ	3.459(5)
$\pi_{Ph}\cdots\pi_{py}$	C8 \cdots C1 ⁱ	3.628(5)
$\pi_{Ph}\cdots\pi_{py}$	C9 \cdots N1 ⁱ	3.581(5)
$\pi_{Ph}\cdots\pi_{py}$	C10 \cdots C5 ⁱ	3.611(6)
$\pi_{Ph}\cdots\pi_{py}$	C11 \cdots C4 ⁱ	3.667(6)
$\pi_{Ph}\cdots\pi_{py}$	C12 \cdots C4 ⁱ	3.619(5)

Table S2. Calculated transitions for [ZnI₂(pyCNPhI)] complex.

Wavelength [nm]	Oscillator strength	Main components	%
436.71	0.0005	HOMO \rightarrow LUMO	99.93
420.75	0.0091	HOMO-1 \rightarrow LUMO	84.57
		HOMO-2 \rightarrow LUMO	14.81
412.42	0.0704	HOMO-2 \rightarrow LUMO	54.17
		HOMO-4 \rightarrow LUMO	22.55
		HOMO-3 \rightarrow LUMO	15.93
		HOMO-1 \rightarrow LUMO	6.65
407.04	0.0110	HOMO-3 \rightarrow LUMO	70.65
		HOMO-4 \rightarrow LUMO	27.73
391.40	0.3832	HOMO-4 \rightarrow LUMO	49.16
		HOMO-2 \rightarrow LUMO	29.00
		HOMO-3 \rightarrow LUMO	12.67
		HOMO-1 \rightarrow LUMO	8.02
345.77	0.0593	HOMO-5 \rightarrow LUMO	99.08
317.26	0.0020	HOMO-6 \rightarrow LUMO	98.97
315.11	0.0080	HOMO-7 \rightarrow LUMO	96.34
297.45	0.0065	HOMO-9 \rightarrow LUMO	89.62
		HOMO-8 \rightarrow LUMO	8.52
290.41	0.0002	HOMO \rightarrow LUMO+1	99.76
287.00	0.1727	HOMO-8 \rightarrow LUMO	83.98
		HOMO-9 \rightarrow LUMO	8.13
283.32	0.0005	HOMO-1 \rightarrow LUMO+1	84.48
		HOMO-2 \rightarrow LUMO+1	14.80
279.32	0.0038	HOMO-3 \rightarrow LUMO+1	48.91
		HOMO-2 \rightarrow LUMO+1	41.50
		HOMO-1 \rightarrow LUMO+1	4.81
		HOMO-4 \rightarrow LUMO+1	2.05
277.30	0.0165	HOMO-3 \rightarrow LUMO+1	34.46

		HOMO-4 → LUMO+1	21.53
		HOMO-2 → LUMO+1	15.84
		HOMO-2 → LUMO+2	10.07
		HOMO-1 → LUMO+2	4.26
		HOMO-1 → LUMO+1	3.04
276.67	0.0021	HOMO-2 → LUMO+2	44.91
		HOMO-1 → LUMO+2	19.46
		HOMO-4 → LUMO+1	11.94
		HOMO-4 → LUMO+2	7.77
		HOMO-3 → LUMO+2	5.71
		HOMO-2 → LUMO+1	1.82
		HOMO-3 → LUMO+1	1.53
271.41	0.0409	HOMO-4 → LUMO+1	56.96
		HOMO-3 → LUMO+1	11.71
		HOMO-2 → LUMO+1	11.28
		HOMO-1 → LUMO+1	5.39
		HOMO-10 → LUMO	2.62
269.19	0.1637	HOMO-10 → LUMO	65.37
		HOMO-12 → LUMO	19.48
		HOMO-11 → LUMO	3.12
		HOMO-2 → LUMO+1	2.97
		HOMO-8 → LUMO	2.87
251.69	0.0144	HOMO-2 → LUMO+3	48.32
		HOMO-1 → LUMO+3	28.81
		HOMO-7 → LUMO+4	7.24
		HOMO-4 → LUMO+3	3.79
		HOMO-3 → LUMO+3	3.25
		HOMO-7 → LUMO+1	2.97
		HOMO-7 → LUMO	2.49
249.13	0.0121	HOMO → LUMO+3	68.58
		HOMO → LUMO+2	22.96
		HOMO → LUMO+4	4.44
		HOMO → LUMO+5	2.49
248.01	0.0261	HOMO-5 → LUMO+1	47.63
		HOMO-12 → LUMO	2.03
247.80	0.0006	HOMO → LUMO+2	70.45
		HOMO → LUMO+3	26.89
244.90	0.0028	HOMO-1 → LUMO+3	46.37
		HOMO-2 → LUMO+3	22.45
		HOMO-1 → LUMO+2	10.59
		HOMO-1 → LUMO+5	4.84
		HOMO-2 → LUMO+2	3.90
		HOMO-2 → LUMO+4	2.49
		HOMO-1 → LUMO+4	2.31
244.55	0.0173	HOMO-11 → LUMO	41.61
		HOMO-12 → LUMO	23.75
		HOMO-10 → LUMO	12.70
		HOMO-2 → LUMO+4	5.54
		HOMO-1 → LUMO+4	3.45
		HOMO-8 → LUMO+1	3.19
242.97	0.0160	HOMO → LUMO+4	78.47
		HOMO → LUMO+5	5.89

		HOMO → LUMO+2	4.92
		HOMO-1 → LUMO+2	3.08
		HOMO → LUMO+3	2.25
242.69	0.0056	HOMO-1 → LUMO+2	51.37
		HOMO-2 → LUMO+2	19.08
		HOMO-1 → LUMO+3	12.03
		HOMO-2 → LUMO+3	5.63
		HOMO → LUMO+4	5.60
		HOMO-6 → LUMO+2	3.22
240.80	0.0003	HOMO-6 → LUMO+2	92.77
240.01	0.0174	HOMO-3 → LUMO+3	30.36
		HOMO-4 → LUMO+3	27.24
		HOMO-3 → LUMO+2	7.36
		HOMO-2 → LUMO+3	6.11
		HOMO-2 → LUMO+4	5.32
		HOMO-4 → LUMO+2	4.61
		HOMO-2 → LUMO+2	2.94
		HOMO-3 → LUMO+4	2.66
		HOMO-1 → LUMO+4	2.57
		HOMO-3 → LUMO+5	2.25
239.10	0.0178	HOMO-4 → LUMO+3	43.11
		HOMO-3 → LUMO+3	19.91
		HOMO-3 → LUMO+2	8.69
		HOMO-1 → LUMO+4	5.71
		HOMO-3 → LUMO+4	4.49
		HOMO-4 → LUMO+2	3.28
		HOMO-3 → LUMO+5	2.99
		HOMO-4 → LUMO+4	2.49
238.47	0.0016	HOMO-1 → LUMO+4	55.76
		HOMO-2 → LUMO+4	12.56
		HOMO-1 → LUMO+5	5.79
		HOMO-1 → LUMO+2	4.95
		HOMO-3 → LUMO+3	3.96
		HOMO-3 → LUMO+2	3.66
		HOMO-4 → LUMO+3	3.47
		HOMO-1 → LUMO+3	3.44
		HOMO-2 → LUMO+3	2.31
		HOMO-2 → LUMO+5	2.02
237.94	0.0125	HOMO-3 → LUMO+2	34.68
		HOMO-3 → LUMO+3	24.94
		HOMO-4 → LUMO+2	19.75
		HOMO-2 → LUMO+2	10.48
236.99	0.0014	HOMO-4 → LUMO+2	51.53
		HOMO-3 → LUMO+2	18.69
		HOMO-4 → LUMO+3	10.26
		HOMO-3 → LUMO+3	7.80
236.69	0.0619	HOMO-2 → LUMO+4	26.49
		HOMO-11 → LUMO	22.77
		HOMO-12 → LUMO	16.41
		HOMO-3 → LUMO+2	12.56
		HOMO-8 → LUMO+1	7.05
		HOMO-10 → LUMO+1	2.70

234.52	0.0131	HOMO-4 → LUMO+4	24.86		
		HOMO-12 → LUMO	16.04		
		HOMO-2 → LUMO+4	15.13		
		HOMO-4 → LUMO+2	6.25		
		HOMO-1 → LUMO+4	5.58		
		HOMO-4 → LUMO+3	4.44		
		HOMO-11 → LUMO	4.23		
		HOMO-10 → LUMO	4.17		
		HOMO-3 → LUMO+4	4.12		
		HOMO-4 → LUMO+5	3.53		
		HOMO-2 → LUMO+5	2.35		
		HOMO-8 → LUMO+1	2.01		
		233.28	0.0237	HOMO-3 → LUMO+4	63.72
				HOMO-4 → LUMO+4	10.52
HOMO → LUMO+5	4.58				
HOMO-3 → LUMO+2	4.47				
HOMO-3 → LUMO+5	3.84				
HOMO-3 → LUMO+3	3.41				
HOMO-4 → LUMO+2	2.54				
232.18	0.0700	HOMO → LUMO+5	81.07		
		HOMO → LUMO+4	7.10		
		HOMO-3 → LUMO+4	4.63		
229.76	0.0008	HOMO-6 → LUMO+1	93.08		
		HOMO-6 → LUMO+4	4.33		
229.36	0.0060	HOMO-1 → LUMO+5	34.07		
		HOMO-4 → LUMO+4	22.96		
		HOMO-1 → LUMO+4	14.02		
		HOMO-2 → LUMO+5	10.89		
		HOMO-12 → LUMO	4.02		
		HOMO-10 → LUMO	2.70		
		HOMO-3 → LUMO+4	2.02		
229.17	0.0286	HOMO-1 → LUMO+5	31.94		
		HOMO-4 → LUMO+4	25.96		
		HOMO-2 → LUMO+4	18.91		
		HOMO-2 → LUMO+5	4.89		
		HOMO-3 → LUMO+4	4.83		
		HOMO-12 → LUMO	4.06		
		HOMO-10 → LUMO	2.94		
224.74	0.0433	HOMO-3 → LUMO+5	42.76		
		HOMO-2 → LUMO+5	20.24		
		HOMO-4 → LUMO+5	12.59		
		HOMO-7 → LUMO+1	6.88		
		HOMO-3 → LUMO+4	5.45		
		HOMO-1 → LUMO+5	3.08		
		HOMO-2 → LUMO+4	2.90		
224.46	0.0227	HOMO-7 → LUMO+1	76.90		
		HOMO-7 → LUMO+2	8.41		
		HOMO-3 → LUMO+5	4.27		
		HOMO-9 → LUMO+1	2.43		
223.53	0.0664	HOMO-4 → LUMO+5	54.24		
		HOMO-3 → LUMO+5	27.27		
		HOMO-4 → LUMO+4	4.68		

		HOMO-2 → LUMO+5	3.52
		HOMO-3 → LUMO+4	3.22
223.09	0.0014	HOMO-7 → LUMO+2	89.23
		HOMO-7 → LUMO+1	7.59
221.33	0.0041	HOMO-9 → LUMO+1	85.12
		HOMO-7 → LUMO+1	3.48
		HOMO-10 → LUMO+1	2.34
		HOMO-8 → LUMO+1	2.14
219.96	0.0007	HOMO-6 → LUMO+3	98.27
216.78	0.0233	HOMO-5 → LUMO+3	92.43
		HOMO-5 → LUMO+2	5.54
216.09	0.0088	HOMO-5 → LUMO+2	80.68
		HOMO-5 → LUMO+3	5.74
		HOMO-5 → LUMO+4	4.27
		HOMO-8 → LUMO+1	3.25
		HOMO-8 → LUMO+2	2.72
214.08	0.0516	HOMO-8 → LUMO+1	49.62
		HOMO-5 → LUMO+4	17.05
		HOMO-5 → LUMO+2	8.15
		HOMO-11 → LUMO	7.62
		HOMO-2 → LUMO+5	2.63
		HOMO-10 → LUMO+1	2.23
213.24	0.0043	HOMO-2 → LUMO+5	45.23
		HOMO-4 → LUMO+5	17.46
		HOMO-1 → LUMO+5	14.63
		HOMO-3 → LUMO+5	11.26
		HOMO-8 → LUMO+1	2.22
211.69	0.0331	HOMO-5 → LUMO+4	54.94
		HOMO-8 → LUMO+2	8.65
		HOMO-13 → LUMO	7.84
		HOMO-14 → LUMO	7.48
		HOMO-8 → LUMO+1	7.22
		HOMO-10 → LUMO+1	4.13
		HOMO-15 → LUMO	2.08
210.43	0.0010	HOMO-6 → LUMO+4	88.52
		HOMO-6 → LUMO+1	4.67
		HOMO-6 → LUMO+6	2.96
210.28	0.0052	HOMO-8 → LUMO+2	70.35
		HOMO-10 → LUMO+2	9.78
		HOMO-5 → LUMO+4	4.41
		HOMO-5 → LUMO+2	4.23
209.52	0.0488	HOMO-13 → LUMO	45.27
		HOMO-14 → LUMO	14.57
		HOMO-5 → LUMO+4	13.21
		HOMO-8 → LUMO+1	9.90
		HOMO-15 → LUMO	8.83
204.94	0.0127	HOMO → LUMO+6	79.96
		HOMO-13 → LUMO	7.28
		HOMO-14 → LUMO	5.98
204.85	0.0436	HOMO-13 → LUMO	25.29
		HOMO-14 → LUMO	23.89
		HOMO → LUMO+6	17.04

		HOMO-8 → LUMO+3	7.89
		HOMO-7 → LUMO+4	5.74
		HOMO-2 → LUMO+6	3.66
		HOMO-15 → LUMO	2.81
		HOMO-10 → LUMO+1	2.29
204.64	0.0266	HOMO-8 → LUMO+3	47.07
		HOMO-7 → LUMO+4	26.84
		HOMO-13 → LUMO	6.12
		HOMO-10 → LUMO+3	5.17
		HOMO-14 → LUMO	3.10
202.84	0.0321	HOMO-10 → LUMO+1	34.05
		HOMO-1 → LUMO+6	23.50
		HOMO-12 → LUMO+1	10.99
		HOMO-2 → LUMO+6	5.95
		HOMO-11 → LUMO+1	5.25
		HOMO-14 → LUMO	3.72
		HOMO-9 → LUMO+1	3.39
201.45	0.0298	HOMO-1 → LUMO+6	62.56
		HOMO-10 → LUMO+1	11.41
		HOMO-14 → LUMO	9.05
		HOMO-12 → LUMO+1	4.32
		HOMO-15 → LUMO	2.46
200.92	0.0302	HOMO-2 → LUMO+6	72.12
		HOMO-5 → LUMO+5	9.20
		HOMO-1 → LUMO+6	7.19
		HOMO-15 → LUMO	3.51
		HOMO-14 → LUMO	2.18
198.84	0.3207	HOMO-5 → LUMO+5	65.98
		HOMO-4 → LUMO+6	10.76
		HOMO-2 → LUMO+6	7.30
		HOMO-1 → LUMO+7	3.05
198.34	0.0079	HOMO-3 → LUMO+6	90.65
		HOMO-15 → LUMO	3.42
197.43	0.1794	HOMO-4 → LUMO+6	42.77
		HOMO-7 → LUMO+3	13.76
		HOMO-15 → LUMO	9.81
		HOMO-5 → LUMO+5	9.34
		HOMO-8 → LUMO+4	9.10
		HOMO-14 → LUMO	4.43
		HOMO-3 → LUMO+6	3.00
197.05	0.1723	HOMO-7 → LUMO+3	38.85
		HOMO-4 → LUMO+6	32.14
		HOMO-8 → LUMO+4	16.11
		HOMO-7 → LUMO+4	2.20
194.34	0.0026	HOMO-15 → LUMO	43.46
		HOMO-14 → LUMO	14.57
		HOMO-16 → LUMO	11.64
		HOMO-8 → LUMO+4	9.15
		HOMO-4 → LUMO+6	7.86
		HOMO-11 → LUMO+1	2.64
193.77	0.0162	HOMO-9 → LUMO+3	92.13
192.94	0.1108	HOMO-8 → LUMO+3	37.43

		HOMO-7 → LUMO+4	37.06
		HOMO-10 → LUMO+3	5.78
		HOMO-9 → LUMO+2	4.69
		HOMO-8 → LUMO+4	2.90
		HOMO-2 → LUMO+3	2.14
192.34	0.0695	HOMO-9 → LUMO+2	65.41
		HOMO-9 → LUMO+4	11.87
		HOMO-7 → LUMO+3	3.32
		HOMO-8 → LUMO+4	3.14
		HOMO-8 → LUMO+3	2.82
		HOMO-9 → LUMO+3	2.82
		HOMO-7 → LUMO+4	2.58
191.10	0.1288	HOMO-8 → LUMO+4	26.67
		HOMO-9 → LUMO+2	22.16
		HOMO-12 → LUMO+1	15.62
		HOMO-9 → LUMO+4	12.39
		HOMO-7 → LUMO+3	8.37
		HOMO-16 → LUMO	3.22
		HOMO-10 → LUMO+1	3.19
189.64	0.0476	HOMO-9 → LUMO+4	63.41
		HOMO-12 → LUMO+1	10.07
		HOMO-8 → LUMO+4	5.18
		HOMO-9 → LUMO+2	4.79
		HOMO-16 → LUMO	3.86
		HOMO-7 → LUMO+3	2.79
		HOMO-11 → LUMO+1	2.02
188.54	0.2109	HOMO-12 → LUMO+1	31.06
		HOMO-10 → LUMO+1	20.53
		HOMO-11 → LUMO+1	11.58
		HOMO-16 → LUMO	8.22
		HOMO-7 → LUMO+3	6.80
		HOMO-8 → LUMO+4	6.41
		HOMO-5 → LUMO+6	3.81

Fig. S3. UV-Vis spectra of $[\text{ZnI}_2(\text{L}^{4-})]$ complex, free L^{4-} ligand, and ZnI_2 in various solvents.

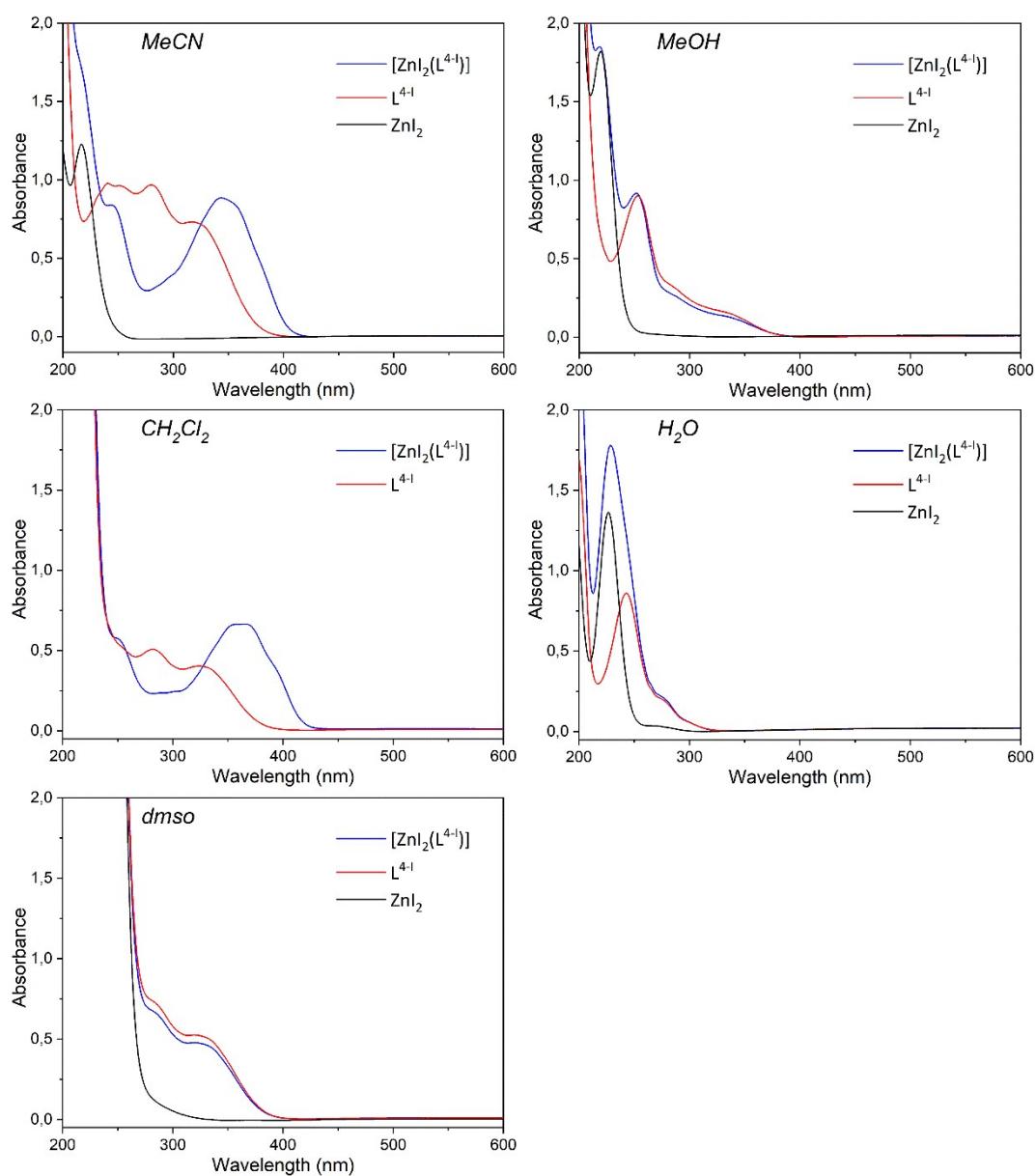


Fig. S4. Experimental (black) and TD-DFT/def2-TZVP/ECP(I)/IEFPCM(acetonitrile) simulated (red vertical lines) UV-Vis spectra of the $[\text{ZnI}_2(\text{L}^{4-})]$ complex (calculated data were scaled by a factor of 0.88).

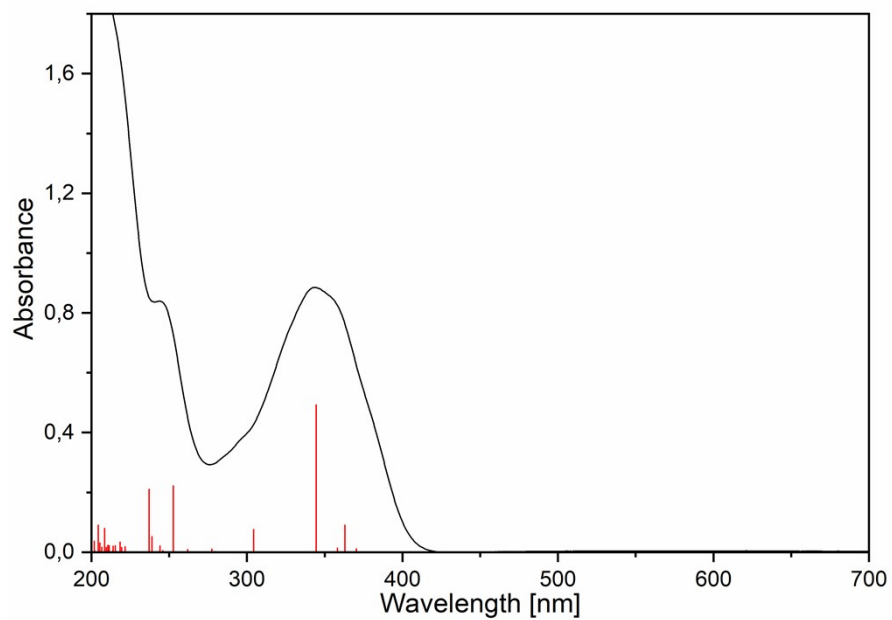


Fig. S5. The ^1H NMR spectrum of $[\text{ZnI}_2(\text{L}^{4-})]$ complex in CD_3CN ($25\text{ }^\circ\text{C}$).

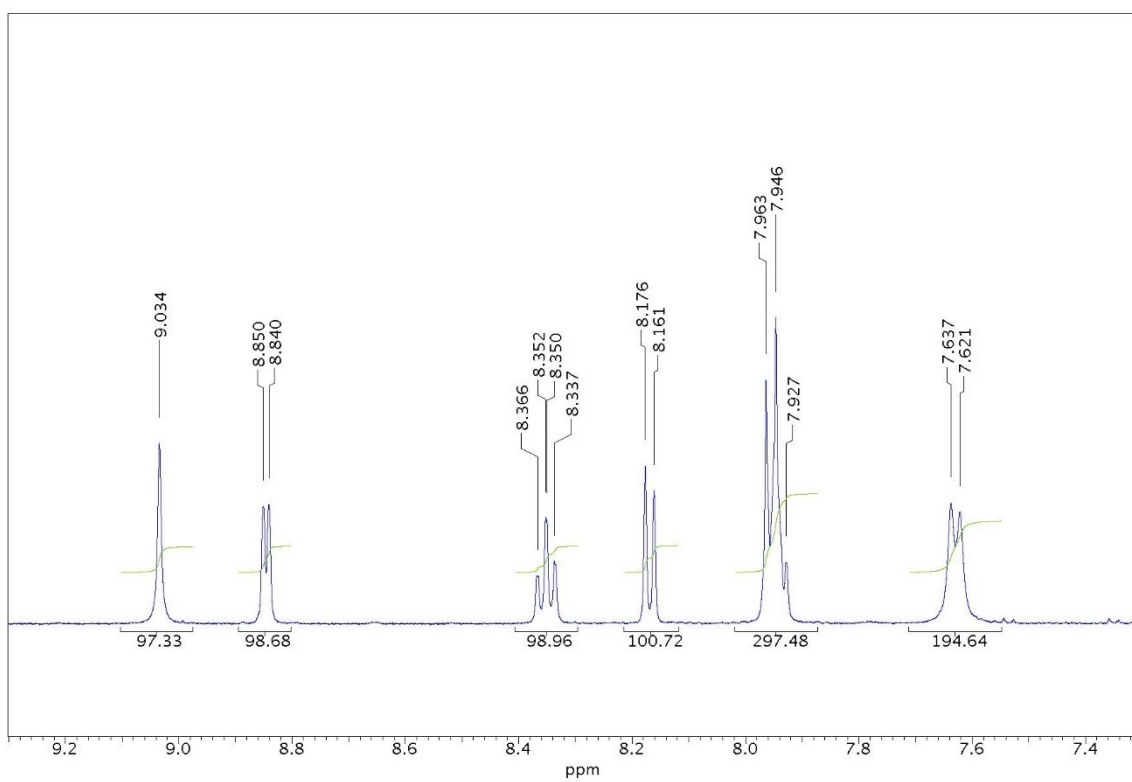
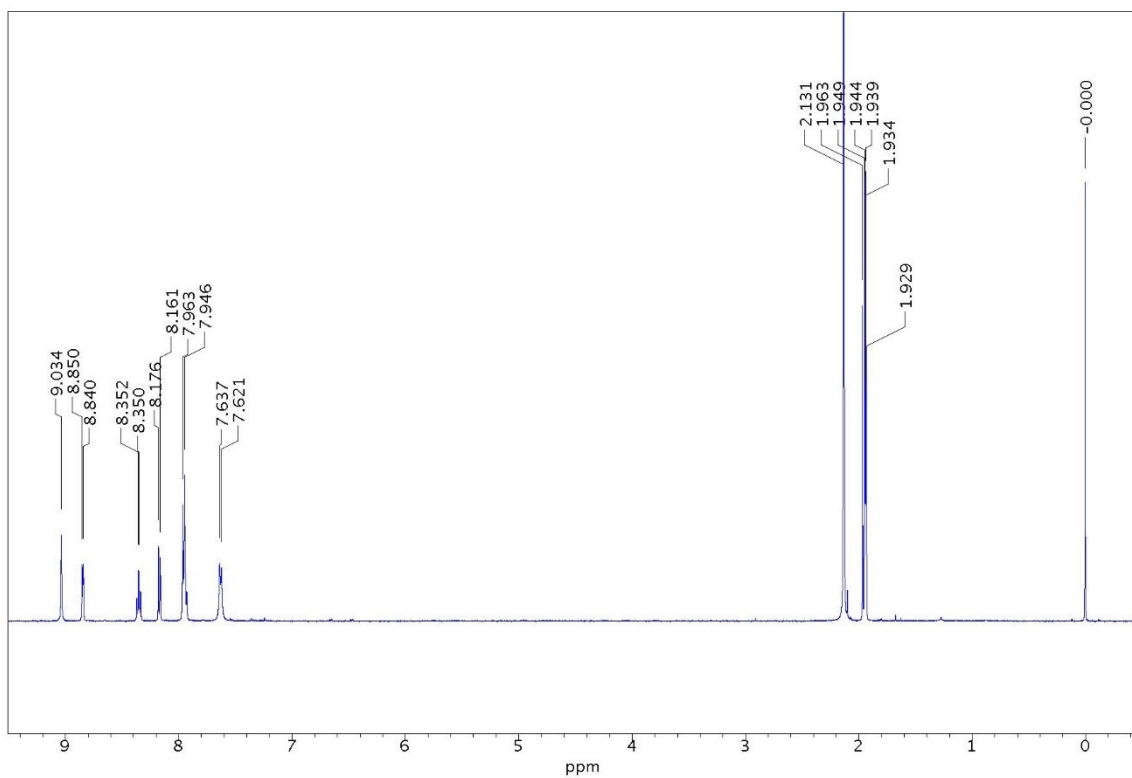


Fig. S6. The ^{13}C NMR spectrum of $[\text{ZnI}_2(\text{L}^{4-1})]$ complex in CD_3CN (temp. $25\text{ }^\circ\text{C}$).

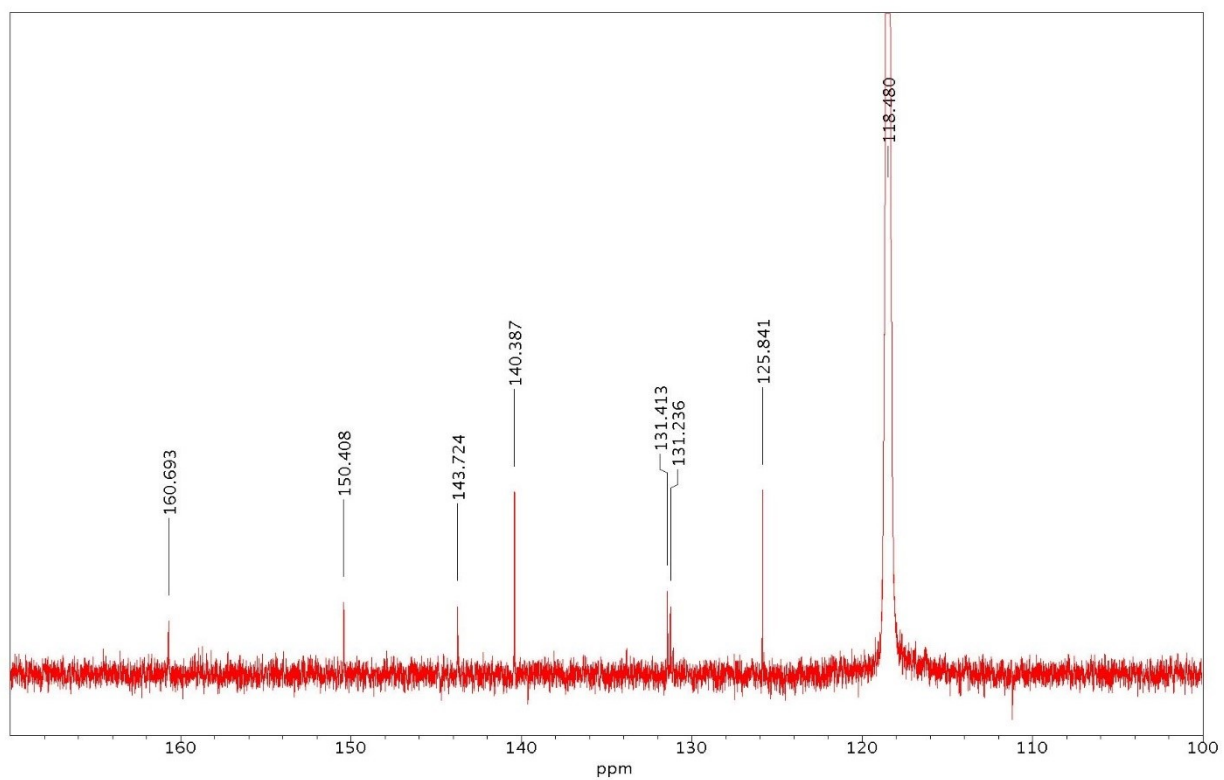


Fig. S7. The ^1H - ^{13}C HMBC spectrum of $[\text{ZnI}_2(\text{L}^{4-})]$ complex in CD_3CN (at 25°C). The ^1H and ^{13}C NMR spectra of the $[\text{ZnI}_2(\text{L}^{4-})]$ complex are presented as projection spectra. The positions of the quaternary carbon atoms' signals: C2 (147.92 ppm), C1'(144.89 ppm), and C4' (96.65 ppm), which were not detected in the 1D ^{13}C NMR spectrum, are marked by the red arrows.

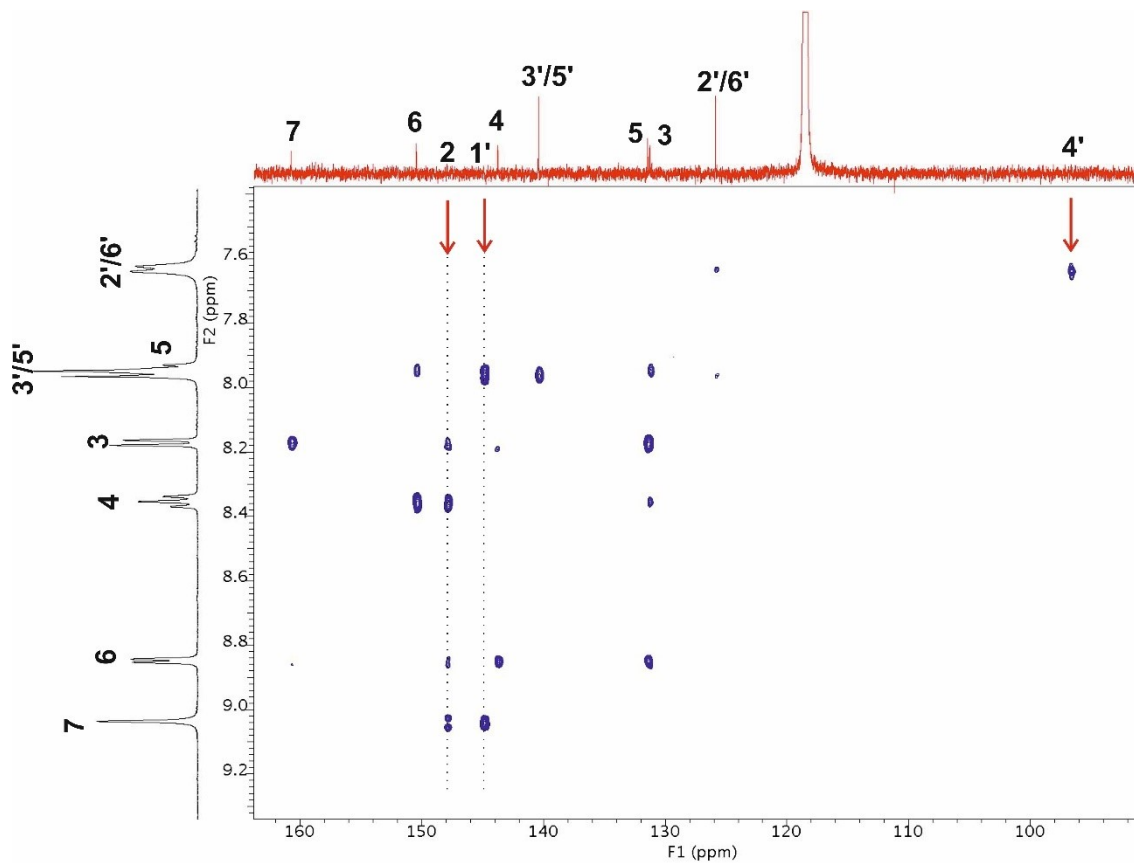


Table S3. The experimental ^1H and ^{13}C NMR chemical shifts δ [ppm] for free L^{4-1} ligand and $[\text{ZnI}_2(\text{L}^{4-1})]$ complex in CD_3CN , (temp. 25 °C, ref. to TMS, solvent: δ (^1H) 1.941 ppm, δ (^{13}C) 1.51 ppm, 118.48 ppm).

Atom labeling	L^{4-1} ligand			$[\text{ZnI}_2(\text{L}^{4-1})]$ complex		
	δ (^1H)*	δ (^{13}C)	^1H - ^{13}C HMBC#	δ (^1H)*	δ (^{13}C)	^1H - ^{13}C HMBC#
2	-	155.58	-	-	147.92 [§]	-
3	8.153 (1H, <i>d</i> , $J_{\text{HH}}=7.9$ Hz)	122.48	H3 \rightarrow C7, C5, C2	8.168 (1H, <i>d</i> , $J_{\text{HH}}=7.8$ Hz)	131.24	H3 \rightarrow C7, C5, C2
4	7.882 (1H, <i>ddd</i> , $J_{\text{HH}}=7.7, 7.7, 1.8$ Hz)	138.07	H4 \rightarrow C6, C2	8.351 (1H, <i>ddd</i> , $J_{\text{HH}}=7.8, 7.8, 1.4$ Hz)	143.72	H4 \rightarrow C6, C2, C3
5	7.451 (1H, <i>ddd</i> , $J_{\text{HH}}=7.5, 4.8, 1.3$ Hz)	126.74	H5 \rightarrow C6, C3	7.940 (1H) overlapping signal	131.41	H5 \rightarrow C6, C3
6	8.695 (1H, <i>d</i> , $J_{\text{HH}}=4.8$ Hz)	151.01	H6 \rightarrow C2, C4, C5	8.845 (1H, <i>d</i> , $J_{\text{HH}}=5.2$ Hz)	150.41	H6 \rightarrow C4, C5, C2
7	8.557 (1H, <i>s</i>)	163.02	H7 \rightarrow C2, C1', C3	9.034 (1H, <i>s</i>)	160.69	H7 \rightarrow C2, C1'
1'	-	152.03	-	-	144.89 [§]	-
2'/6'	7.086 (2H, <i>d</i> , $J_{\text{HH}}=8.6$ Hz)	124.49	H2'/H6' \rightarrow C4', C2'/6', C3'/5', C1'	7.629 (2H, <i>d</i> , $J_{\text{HH}}=8.3$ Hz)	125.84	H2'/H6' \rightarrow C4', C2'/6'
3'/5'	7.769 (2H, <i>d</i> , $J_{\text{HH}}=8.6$ Hz)	139.49	H3'/H5' \rightarrow C1', C3'/5', C4', C2'/6'	7.955 (2H) overlapping signal	140.39	H3'/H5' \rightarrow C1', C3'/5'
4'	-	91.75	-	-	96.65 [§]	-

*in brackets (multiplicity, number of protons, proton-proton coupling constants J_{HH} [Hz]);

the heteronuclear multiple bond diagnostic correlation between the given carbon atoms and the showing proton(s) are presented;

[§] chemical shifts of quaternary carbon atoms signals were detected in ^1H - ^{13}C HMBC spectrum.

Fig. S8. XANES spectra of the $[\text{ZnI}_2(\text{L}^{4-1})]$ complex registered in solid state (black line, no offset) and in various solvents: DMPU (brown line, offset 0.2), CH_2Cl_2 (purple, offset 0.4), acetonitrile (blue line, offset 1.0), methanol (orange line, offset 1.3), water (green line, offset 1.6), and DMSO (red line offset 2.0).

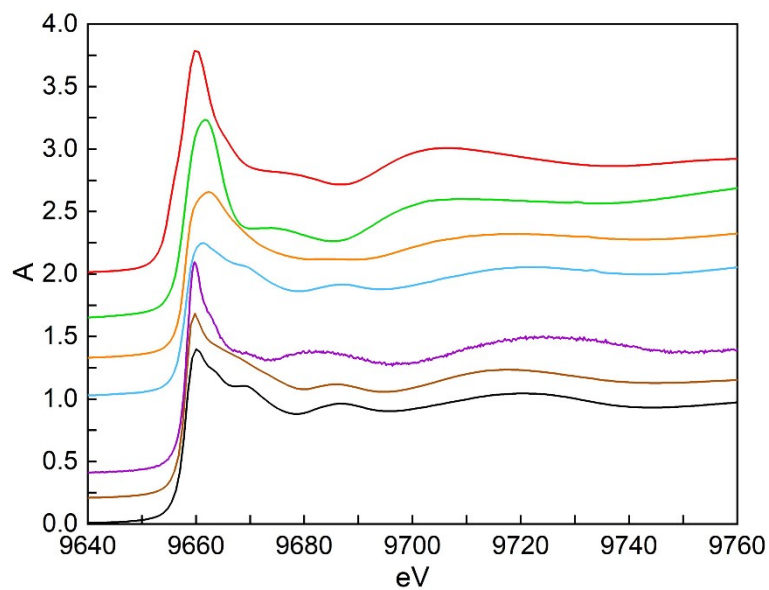


Table S4. MICs/MBC values (mg/L) and zone diameters of bacterial growth inhibition (mm) * obtained for test compounds and ciprofloxacin for reference strains.

Compound	<i>E. coli</i> ATCC25922		<i>P. aeruginosa</i> ATCC27853		<i>S. aureus</i> ATCC29213		<i>S. aureus</i> ATCC6538		<i>E. faecalis</i> ATCC29212	
	MIC (mg/L)	Zone diameter (mm)	MIC (mg/L)	Zone diameter (mm)	MIC (mg/L)	Zone diameter (mm)	MIC (mg/L)	Zone diameter (mm)	MIC (mg/L)	Zone diameter (mm)
ZnCl ₂	512	ND	>512	ND	256	ND	512	ND	256	ND
ZnI ₂	512	ND	>512	ND	512	ND	512	ND	512	ND
L ⁴⁺	>512	6	>512	6	>512	6	>512	6	>512	6
[ZnCl ₂ (L ⁴⁺)]	512	6	>512	6	>512	6	>512	6	>512	6
[ZnI ₂ (L ⁴⁺)]	512	6	>512	6	>512	6	>512	6	>512	6
Ciprofloxacin	<0,5	35	<0,5	32	<0,5	25	<0,5	25	1	23

*ND: No data available.